

Airy-Gauss beams and their transformation by paraxial optical systems

Miguel A. Bandres¹ and Julio C. Gutiérrez-Vega^{2*}

¹California Institute of Technology, Pasadena, California 91125, USA

²Photonics and Mathematical Optics Group, Tecnológico de Monterrey, México, 64849

[*juliocesar@itesm.mx](mailto:juliocesar@itesm.mx)

Abstract: We introduce the generalized Airy-Gauss (AiG) beams and analyze their propagation through optical systems described by ABCD matrices with complex elements in general. The transverse mathematical structure of the AiG beams is form-invariant under paraxial transformations. The conditions for square integrability of the beams are studied in detail. The AiG beam describes in a more realistic way the propagation of the Airy wave packets because AiG beams carry finite power, retain the nondiffracting propagation properties within a finite propagation distance, and can be realized experimentally to a very good approximation.

© 2007 Optical Society of America

OCIS codes: (050.1940) Diffraction; (260.1960) Diffraction theory; (070.2590) ABCD transforms; (350.500) Propagation.

References and links

1. H. Kogelnik and T. Li, "Laser beams and resonators," *Proc. IEEE*, **54**, 1312–1329 (1966).
2. A. E. Siegman, *Lasers* (University Science, Mill Valley CA, 1986).
3. E. G. Kalnins and W. Miller Jr., "Lie theory and separation of variables. 5. The equations $iU_t + U_{xx} = 0$ and $iU_t + U_{xx} - c/x^2 U = 0$," *J. Math. Phys.* **15**, 1728–1737 (1974).
4. M. V. Berry and N. L. Balazs, "Nonspreading wave packets," *Am. J. Phys.* **47**, 264–267 (1979).
5. I. M. Besieris, A. M. Shaarawi, and R. W. Ziolkowski, "Nondispersive accelerating wave packets," *Am. J. Phys.* **62**, 519–521 (1994).
6. K. Unnikrishnan and A. R. P. Rau, "Uniqueness of the Airy Packet in quantum mechanics," *Am. J. Phys.* **64**, 1034–1036 (1996).
7. G. A. Siviloglou and D. N. Christodoulides, "Accelerating finite energy Airy beams," *Opt. Lett.* **32**, 979–981 (2007).
8. I. M. Besieris and A. M. Shaarawi, "A note on an accelerating finite energy Airy beam," *Opt. Lett.* **32**, 2447–2449 (2007).
9. G. A. Siviloglou, J. Broky, A. Dogariu, and D. N. Christodoulides, "Observation of accelerating Airy beams," *Phys. Rev. Lett.* **99**, 213901 (2007).
10. H. M. Osaktas, Z. Zalevski, and M. A. Kutay, *The Fractional Fourier Transform with applications in Optics and Signal processing* (Wiley, London, 2001).
11. M. Abramowitz and I.A. Stegun, *Handbook of mathematical functions* (Dover, New York, 1964).
12. O. Vallée and M Soares, *Airy functions and applications to physics* (Imperial College Press, London, 2004).

1. Introduction

Theoretical and experimental studies of the spatial structure of laser beams have been subjects of continuing interest and research since the early years of laser physics [1]. Paraxial propagation of scalar optical fields in planar geometries is described by the (1+1)D paraxial wave equation (PWE)

$$\left(\frac{\partial^2}{\partial x^2} + i2k\frac{\partial}{\partial z}\right)U(x,z) = 0, \quad (1)$$

where k is the wave number in the propagation medium, and (x,z) are the transverse and longitudinal coordinates, respectively. The most familiar solutions to Eq. (1) are the Hermite-Gaussian beams, whose mathematical and physical properties are well known [2]. Three-dimensional solutions of the (2+1)D PWE can be readily constructed with products of planar solutions, i.e. $U(x,y,z) = U_x(x,z)U_y(y,z)$.

Solutions to Eq. (1) in terms of Airy functions were analyzed independently by Kalnins and Miller in 1974 and by Berry and Balazs in 1979 within the context of quantum mechanics [3, 4]. In these seminal papers, the field across the plane $z = 0$ is assumed to have the form $U(x,0) = \text{Ai}(bx)$, where Ai denotes the Airy function and b is a real and positive constant. The Airy beams lack parity symmetry about the origin, propagate in free space without distortion, and exhibit a peculiar parabolic transverse shift with propagation distance. The existence of this lateral shift motivated Berry and Balazs to adopt the term *accelerating* for describing the Airy wave packets. Some mathematical and physical properties of the Airy wave packets were further explored by Besieris et al. [5] and Unnikrishnan et al. [6].

The original Airy beam introduced by Berry and Balazs contains infinite energy. In a recent Letter, Siviloglou and Christodoulides [7] extended the model by introducing a *finite-energy Airy beam* whose distribution at $z = 0$ is given by $U(x,0) = \text{Ai}(bx)\exp(ax)$, with a being a positive real quantity in order to ensure square integrability of the beam. By employing the Fourier decomposition of plane waves, Siviloglou and Christodoulides derived a closed-form expression for the propagation of the finite-energy Airy beams in free space, and also showed that these beams still exhibit the distinctive parabolic lateral shift with propagation distance. More recently, Besieris and Shaarawi [8] provided insight into the dynamics of the finite-energy Airy beams by confirming that, in spite of the transverse shift, the centroid of the beam propagates in a straight line parallel to the z axis, and the beam variance (i.e. the second-order moment) increases quadratically with propagation distance. The first experimental generation of Airy beams was reported recently by Siviloglou et al. in Ref. [9].

In this paper we introduce a generalized form of the Airy beams that will be referred to as Airy-Gaussian (AiG) beams. For the sake of generality, we analyze first the propagation of AiG beams through complex optical ABCD systems, and later we specialize the general results to several special cases. This general approach will allow us to study the propagation of the AiG beams, not only in free space, but also through more general types of paraxial optical systems characterized by complex ABCD matrices, including lenses, Gaussian apertures, cascaded paraxial systems, and systems having quadratic amplitude as well as phase variations about the optical axis.

The AiG beam describes in a more realistic way the propagation of the Airy beams because AiG beams carry finite power, retain the nondiffracting propagation properties within a finite propagation distance, and can be realized experimentally to a very good approximation. The analysis of the first-order moment of the AiG beam confirms that the position of its centroid through the ABCD system follows the ray trajectory predicted by the geometrical optics. We also study the required conditions for ensuring square integrability of the AiG beam. The Airy beams introduced by Berry and Balazs [4] and the finite-energy Airy beams introduced by Siviloglou and Christodoulides [7] are special cases of the AiG beams.

2. Airy-Gaussian beams through ABCD systems

We start the analysis by defining the transverse field of an Airy-Gaussian beam at the input plane (x_1, z_1) of a first-order optical ABCD system as

$$U_1(x_1; \kappa_1, \delta_1, S_1, q_1) = \text{Ai}\left(\frac{x_1 + \delta_1}{\kappa_1}\right) \exp\left[iS_1\left(\frac{x_1 + \delta_1}{\kappa_1}\right) + i\frac{1}{3}S_1^3\right] \exp\left(\frac{ikx_1^2}{2q_1}\right), \quad (2)$$

where the parameters κ_1 , δ_1 , S_1 , and q_1 are complex quantities in the most general situation. The scaling parameter κ_1 controls the spatial frequency of the transverse field oscillations. The parameter S_1 allows for the possibility that the input field U_1 has a transverse decay and tilt. The complex beam parameter q_1 provides an initial Gaussian apodization and spherical wavefront [2]. The parameter δ_1 introduces an optional lateral shift in the Airy function and in the linear phase term, but it does not affect the Gaussian modulation. The overall amplitude factor $\exp(iS_1^3/3)$ is included for later convenience. Equation (2) reduces to the finite-energy Airy beams [7] when $\delta_1 = 0$ and $q_1 = \infty$, and further to the Airy beams [4] if additionally $S_1 = 0$.

Paraxial propagation of the input Airy-Gaussian field $U_1(x_1)$ through the ABCD system can be performed with the Huygens diffraction integral [2]

$$U_2(x_2) = \sqrt{\frac{k}{i2\pi B}} \int_{-\infty}^{\infty} U_1(x_1) \exp\left[\frac{ik}{2B}(Ax_1^2 - 2x_1x_2 + Dx_2^2)\right] dx_1, \quad (3)$$

where $U_2(x_2)$ is the field at the output plane (x_2, z_2) . The integration yields

$$U_2(x_2; \kappa_2, \delta_2, S_2, q_2) = \text{Ai}\left(\frac{x_2 + \delta_2}{\kappa_2}\right) \exp\left[iS_2\left(\frac{x_2 + \delta_2}{\kappa_2}\right) + i\frac{1}{3}S_2^3\right] \text{GB}(x_2, q_2), \quad (4)$$

where

$$\text{GB}(x_2, q_2) = \frac{1}{\sqrt{A + B/q_1}} \exp\left(i\frac{kx_2^2}{2q_2}\right), \quad (5)$$

is the output field of a Gaussian beam with input parameter q_1 travelling axially through the ABCD system, and the transformation laws for the parameters q_2 , κ_2 , S_2 , and δ_2 , from the input plane z_1 to the output plane z_2 are

$$\begin{aligned} q_2 &= \frac{Aq_1 + B}{Cq_1 + D}, & \kappa_2 &= \kappa_1 (A + B/q_1), \\ S_2 &= S_1 + \frac{B}{2k\kappa_1\kappa_2}, & \delta_2 &= \delta_1 (A + B/q_1) - \frac{B}{2k\kappa_1} (S_1 + S_2). \end{aligned} \quad (6)$$

Equations (4)-(6) represent the main result of this study. They permit an arbitrary Airy-Gaussian beam to be propagated in closed-form through a real or complex ABCD optical system. Apart from an overall amplitude factor, the output field has the same mathematical structure as the input field, thus the Airy-Gaussian beams belong to the class of fields whose form is invariant under paraxial optical transformations. This form-invariance property does not have to be confused with the shape-invariance property of the Hermite-Gauss beams which preserve, except for a scaling factor, the same transverse shape under paraxial transformations. In general the shape of the Airy-Gaussian beams will change because κ_1 and κ_2 are not proportional to each other through a real factor leading to different intensity profiles of the function U , and moreover because the parameters q_1 and κ_1 are transformed according to different laws.

We end this section by noting that Eqs. (4)-(6) can be applied to propagate the finite-energy Airy beams studied in Refs. [7, 8] through paraxial ABCD systems. This is achieved by setting

$\delta_1 = 0$ and $q_1 = \infty$, namely

$$U_2(x_2) = \text{Ai}\left(\frac{x_2 + \delta_2}{\kappa_1 A}\right) \exp\left[iS_2\left(\frac{x_2 + \delta_2}{\kappa_1 A}\right) + i\frac{1}{3}S_2^3\right] \frac{1}{\sqrt{A}} \exp\left(i\frac{Ckx_2^2}{2A}\right), \quad (7)$$

where

$$S_2 = S_1 + \frac{B}{2k\kappa_1^2 A}, \quad \delta_2 = -\frac{B}{k\kappa_1} \left(S_1 + \frac{B}{4k\kappa_1^2 A}\right). \quad (8)$$

Furthermore, Eq. (7) represents also the propagation of the Airy beams introduced by Berry and Balazs [4], provided that $S_1 = 0$ in Eqs. (8).

3. Physical discussion

In Section 2 we have demonstrated that generalized Airy-Gaussian beams can be propagated through an ABCD optical system in a closed form. To examine the propagation details of the Airy-Gaussian beams, in this section we study two physically interesting special cases.

3.1. Free space propagation

Let us consider an Airy-Gaussian beam $U(x, z)$ traveling into the half-space $z \geq 0$. The field at the input plane $z = 0$ is given by Eq. (2) and the ABCD transfer matrix for free space propagation from the plane $z_1 = 0$ to the plane $z_2 = z$ reads as $[A, B; C, D] = [1, z; 0, 1]$. The propagated field is given by Eq. (4), where from Eqs. (6) the beam parameters depend on z as follows:

$$\begin{aligned} q_2(z) &= q_1 \mu, & \kappa_2(z) &= \kappa_1 \mu, \\ S_2(z) &= S_1 + \left(\frac{1}{2k\kappa_1^2}\right) \frac{z}{\mu}, & \delta_2(z) &= \delta_1 + \left(\frac{\delta_1}{q_1} - \frac{S_1}{k\kappa_1}\right) z - \left(\frac{1}{4k^2\kappa_1^3}\right) \frac{z^2}{\mu}, \end{aligned} \quad (9)$$

where $\mu = \mu(z) \equiv 1 + z/q_1$.

Figure 1 shows propagations of AiG beams with five different initial parameters up to a distance of $0.2z_R$, where $z_R = kw_1^2/2$ is the Rayleigh distance associated to the initial Gaussian modulation of width w_1 . The corresponding cross sections of the amplitude and phase profiles at the plane $z = 0$ are included at the left side of the Fig. 1. For all examples the scaling parameter κ_1 is assumed real and equal to $w_1/6$. The field distributions $U(x, z)$ were obtained by calculating Eq. (4) using Eq. (9) at 200 transverse planes evenly spaced from the input to the output plane.

The first-order moment (i.e., the expected value of x)

$$x_c(z) = \langle x(z) \rangle = \frac{\int_{-\infty}^{\infty} x |U(x, z)|^2 dx}{\int_{-\infty}^{\infty} |U(x, z)|^2 dx}, \quad (10)$$

gives the centroid of the beam as a function of propagation distance. Although the typical lateral shift of the envelope of the AiG beam can be clearly seen in Fig. 1(a), the position of the centroid remains constant on propagation through free space. The centroid trajectories were obtained by evaluating numerically Eq. (10) at each plane z employing a Gaussian-Legendre quadrature method.

To ensure the shape invariant behavior of the AiG beam, the Gaussian apodization should be large (i.e. $1/q_1 \sim 0$) and $(S_1/k\kappa_1)$ negligible. Under these conditions, the interpretation of the AiG beam as accelerating, i.e., one characterized by a nonlinear lateral shift with range, depends on the z^2 term of the displacement parameter $\delta_2(z)$ in Eq. (9). For small values of $|\kappa_1|$, such as those considered in Refs. [7, 8], the AiG beam exhibit a nonlinear lateral shift at least up to a range where the beam remains essentially diffraction free.

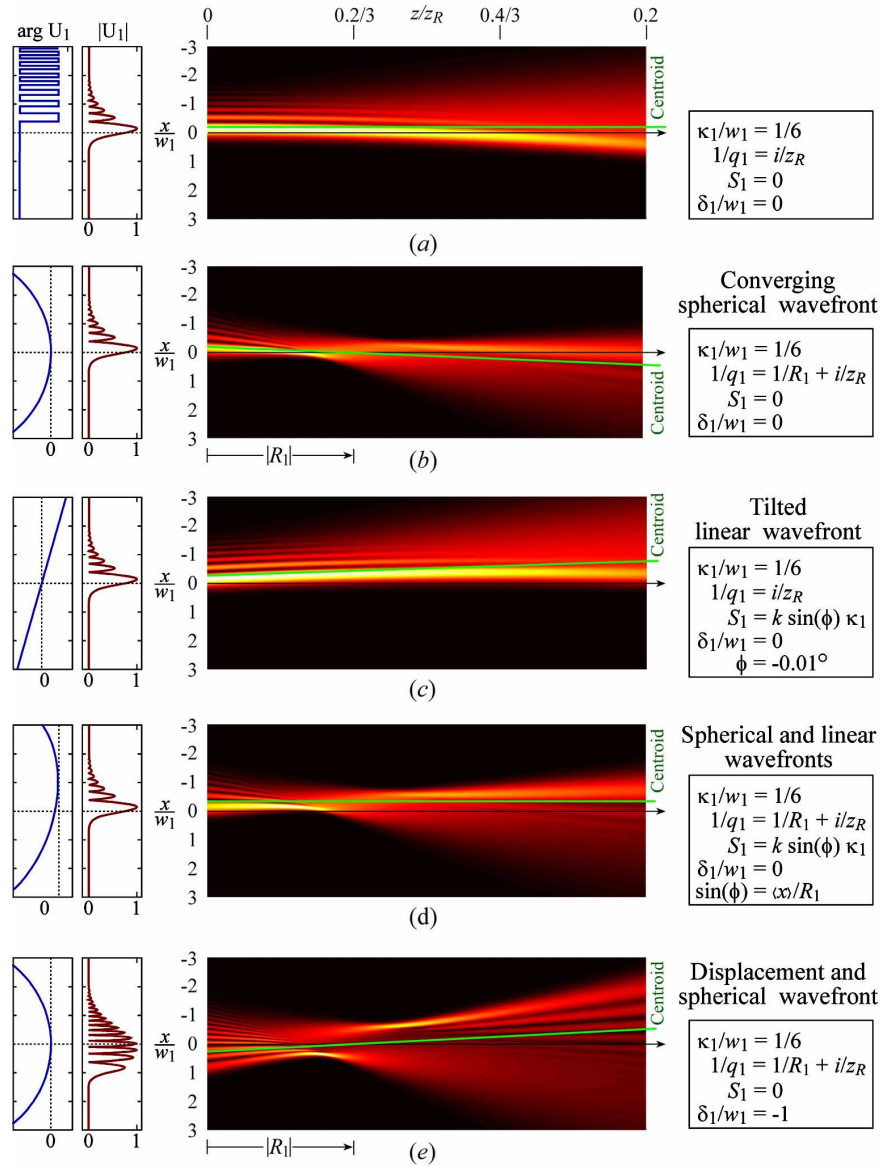


Fig. 1. Free space propagation of an Airy-Gaussian beam for several initial conditions.

To visualize the effect of the beam parameters on the propagation of the AiG beams, let us rewrite the input field [Eq. (2)] as

$$U(x, 0) \propto \text{Ai}\left(\frac{x + \delta_1}{\kappa_1}\right) \exp[(\alpha + i\beta)x] \exp\left(-\frac{x^2}{w_1^2}\right) \exp\left(i\frac{kx^2}{2R_1}\right), \quad (11)$$

where $\alpha = -\text{Im}(S_1/\kappa_1)$ is the linear decay constant, $\beta = \text{Re}(S_1/\kappa_1)$ is the tilt transverse wave number, $R_1 = 1/\text{Re}(q_1^{-1})$ is the radius of curvature of the initial spherical phase front ($R_1 < 0$ convergent phase front, $R_1 > 0$ divergent phase front), and $w_1 = \sqrt{2/k\text{Im}(q_1^{-1})}$ is the $1/e$ amplitude spot size of the Gaussian modulation.

Figure 1(b) shows the propagation of the AiG beam with an initial converging spherical wavefront of radius $R_1 = -(0.2z_R)/3$. Since the quadratic phase factor $\exp(ikx^2/2R_1)$ can be interpreted as the transmittance of a lens of focal distance $f = |R_1|$, Fig. 1(b) represents also the focusing evolution of the initial field in Fig. 1(a). The propagation of the beam centroid exactly follows the geometrical path, as expected from the ray optics approach [2]. The presence of the quadratic phase factor introduces a transverse momentum such that the centroid shifts laterally on propagation following the linear trajectory $x_c(z) = x_c(0)(1 + z/R_1)$, where $x_c(0)$ is the centroid position at the initial plane $z = 0$. Note that R_1 is negative for a converging initial wavefront, then in this case $x_c(z) = 0$ when $z = |R_1|$.

The effect of the initial tilt $\exp(i\beta x)$ is shown in Fig. 1(c). The linear phase transmittance deflects the centroid by an angle ϕ that is related to the tilt transverse wave number β by $\beta = k \sin \phi \approx k\phi$, where k is the wave number and the paraxial approximation $\sin \phi \approx \tan \phi \approx \phi$ has been invoked. On free space propagation, the centroid moves linearly according to $x_c(z) = x_c(0) + \beta z/k$.

The combined effects of the spherical phase front and the linear tilt are shown in Fig. 1(d). Taking into account both effects, the equation for the linear trajectory of the centroid becomes

$$x_c(z) = x_c(0) + \left(\frac{x_c(0)}{R_1} + \frac{\beta}{k} \right) z \quad z \geq 0. \quad (12)$$

For the example shown in Fig. 1(d), the parameters have been chosen such the slope $x_c(0)/R_1 + \beta/k$ vanishes, thus the position of the centroid remains constant on propagation. Finally, the effect of the displacement δ_1 and an initial converging spherical wavefront ($R_1 < 0$) is shown in Fig. 1(e), where we can see that although the initial intensity pattern and its centroid position have changed, the centroid trajectory is still linear and crosses the optical axis at the equivalent focal plane $z = |R_1|$.

We end this section by mentioning that for the special case of free-space propagation, the AiG beam with $\delta_1 = 0$ and $q_1 = \infty$ can be derived using the symmetry properties of the PWE [Eq. 1]. Specifically, given the fundamental Gaussian solution $\text{GB}(x, z)$ to the PWE, then $H(x, z) = \text{GB}(x, z)F(x/\mu, z/\mu)$ is also a solution provided that $F(x, z)$ is a solution to the PWE. Choosing $F(x, z)$ to be the finite energy Airy beam given in Ref. [7], results in an AiG beam propagating in free space.

3.2. Propagation through a quadratic index medium

Let us consider now the propagation of the AiG beams through a graded refractive-index (GRIN) medium with quadratic index variation $n(r) = n_0(1 - x^2/2a^2)$. The ABCD transfer matrix from plane $z_1 = 0$ to plane $z_2 = z$ is given by

$$\begin{bmatrix} A & B \\ C & D \end{bmatrix} = \begin{bmatrix} \cos(z/a) & a \sin(z/a) \\ -\sin(z/a)/a & \cos(z/a) \end{bmatrix}. \quad (13)$$

For a general input AiG field of the form given by Eq. (2), the propagated AiG field at a distance z is described by Eq. (4). Substitution of the matrix elements in Eq. (13) into Eqs. (6)

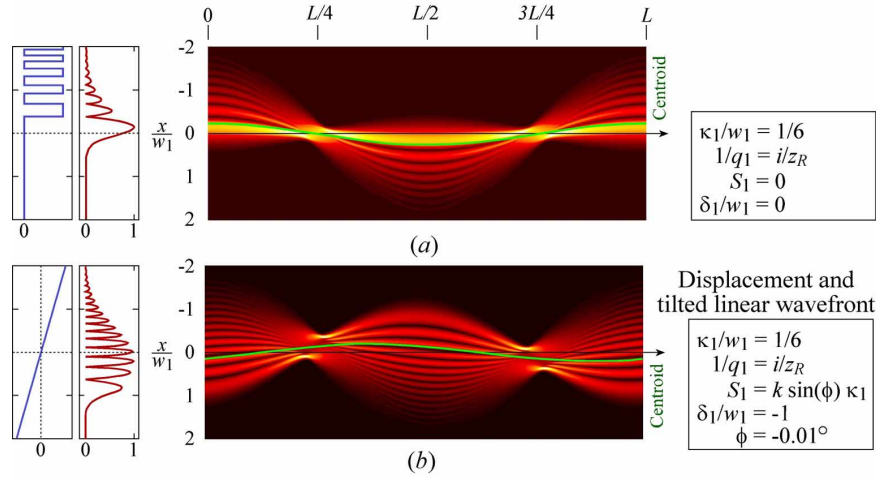


Fig. 2. Propagation of an AiG beam through a GRIN medium for two different initial conditions.

yields the parameter transformations:

$$\begin{aligned}
 q_2(z) &= a \frac{q_1 \cos(z/a) + a \sin(z/a)}{-q_1 \sin(z/a) + a \cos(z/a)}, \\
 \kappa_2(z) &= \kappa_1 [\cos(z/a) + (a/q_1) \sin(z/a)], \\
 S_2(z) &= S_1 + \frac{a}{2k\kappa_1^2 [\cot(z/a) + a/q_1]}, \\
 \delta_2(z) &= \delta_1 \left[\cos\left(\frac{z}{a}\right) + \frac{a \sin(z/a)}{q_1} \right] - \frac{a \sin(z/a)}{2k\kappa_1} (S_1 + S_2),
 \end{aligned} \tag{14}$$

where we note that, under propagation, the beam parameters vary periodically with a longitudinal period $L = 2\pi a$, therefore, the initial field self-reproduces after a distance L .

For a propagation distance $z = L/4 = \pi a/2$, the ABCD matrix Eq. (13) reduces to $[0, a; -1/a, 0]$ which is indeed identical to the matrix transformation from the first to the second focal plane of a converging thin lens of focal length a , i.e. a Fourier transformer. From Eqs. (14) we see that at the Fourier plane $z = L/4$ the beam parameters become

$$\begin{aligned}
 q_2(L/4) &= -a^2/q_1, & \kappa_2(L/4) &= \kappa_1 a/q_1, \\
 S_2(L/4) &= S_1 + \frac{q_1}{2k\kappa_1^2}, & \delta_2(L/4) &= \delta_1 \frac{a}{q_1} - \frac{a}{k\kappa_1} \left(S_1 + \frac{q_1}{4k\kappa_1^2} \right).
 \end{aligned} \tag{15}$$

The Fourier transform $\tilde{U}_1(k_x) = \int_{-\infty}^{\infty} U_1(x) \exp(-ik_x x) dx$ of the AiG beam $U_1(x)$ in Eq. (2) can be determined by inserting Eqs. (15) into Eq. (4) and making the replacements $x \rightarrow k_x$ and $a \rightarrow k$. In a similar way, for intermediate planes $z = pL/4$, the substitution of Eqs. (14) into Eq. (4) yields the p th fractional Fourier transform of the initial field [10].

Figure 2(a) shows the propagation of an AiG beam in a GRIN medium through a distance L . As predicted by geometric optics, the centroid oscillates back and forth across the optical axis following a cosine trajectory with a zero initial slope. The combined effect of an initial tilt and a lateral shift δ_1 is shown in Fig. 2(b). For this case the initial slope of the centroid trajectory is determined by the angle tilt and then the centroid does not cross the Fourier plane at the optical axis.

4. Analysis of the square integrability

From a physical point of view, it is important to identify the range of values of the beam parameters for which the AiG beams transport finite power, i.e. for which the AiG beams are square integrable across the whole transverse plane.

Physical insight is gained by studying the amplitude and phase of the Airy function $\text{Ai}(w)$ on the complex plane $w = u + iv$ as shown in Fig. 3. As the radius $|w|$ increases, the amplitude of the Airy function $|\text{Ai}(w)|$ decreases monotonically in the sector defined by $|\arg w| < \pi/3$, increases indefinitely in the sector $\pi/3 \leq |\arg w| < \pi$, and oscillates with a decreasing average along the negative real axis $\arg w = \pi$. Zeros of the Airy function in the complex plane are located on the negative part of the real axis.

From Eqs. (2) and (4), we know that, at any transverse plane, the AiG beams are proportional to

$$U(x) \propto \text{Ai}\left(\frac{x+\delta}{\kappa}\right) \exp\left(\frac{iS}{\kappa}x\right) \exp\left(\frac{ikx^2}{2q}\right), \quad (16)$$

where the subscripts and overall constants have been omitted for brevity. For given δ and κ , each value of $x \in (-\infty, \infty)$ determines a point $[u(x), v(x)]$ on the complex plane $w = u + iv = (x + \delta)/\kappa$. The parametric equations for $u(x)$ and $v(x)$ are given by

$$w = \frac{x+\delta}{\kappa} = u(x) + iv(x) = \left[\frac{x \text{Re } \kappa + (\kappa \cdot \delta)}{|\kappa|^2} \right] + i \left[\frac{-x \text{Im } \kappa + (\kappa \times \delta)}{|\kappa|^2} \right] \quad (17)$$

where $(\kappa \cdot \delta) \equiv \text{Re } \kappa \text{Re } \delta + \text{Im } \kappa \text{Im } \delta$, and $(\kappa \times \delta) \equiv \text{Re } \kappa \text{Im } \delta - \text{Im } \kappa \text{Re } \delta$. By combining $u(x)$ and $v(x)$ to eliminate x , we obtain that the point $[u(x), v(x)]$ falls on the straight line

$$v_s(u) = -\left(\frac{\text{Im } \kappa}{\text{Re } \kappa}\right)u + \left[\frac{(\text{Im } \kappa / \text{Re } \kappa)(\kappa \cdot \delta) + (\kappa \times \delta)}{|\kappa|^2} \right], \quad (18)$$

Figure 3(d) shows $v_s(u)$ on the plane (u, v) for the case $\text{Re } \kappa > 0$ and $\text{Im } \kappa > 0$.

Let us now to determine the asymptotic expressions of the intensity $|U(x)|^2$ for large values of $|x|$. Useful asymptotic representations of the Airy functions for large argument are given by [11, 12]:

$$\text{Ai}(w) \sim \frac{\exp(-2w^{3/2}/3)}{2\sqrt{\pi}w^{1/4}}, \quad |\arg w| < \pi, \quad (19)$$

$$\text{Ai}(-w) \sim \frac{\sin(2w^{3/2}/3 + \pi/4)}{\sqrt{\pi}w^{1/4}}, \quad |\arg w| < 2\pi/3. \quad (20)$$

Because Eq. (19) does not hold along the negative real axis, we need to deal with the following two cases separately:

1. When the straight line $v_s(u)$ coincides with the real axis $v = 0$. From Eq. (18) we see that this condition is fulfilled when $\text{Im } \kappa = 0$ and $\text{Im } \delta = 0$, and therefore the argument of the Airy function becomes purely real, i.e. $w \in \mathbb{R}$. Applying Eqs. (19) and (20) we obtain for $\text{Re } \kappa > 0$

$$|U|_{x \rightarrow +\infty}^2 \sim \frac{\exp(2\alpha x)}{|x + \text{Re } \delta|^{1/2}} \exp\left[-k \text{Im}\left(\frac{1}{q}\right)x^2\right] \exp\left(-\frac{4}{3}\left|\frac{x + \text{Re } \delta}{\text{Re } \kappa}\right|^{3/2}\right), \quad (21)$$

$$|U|_{x \rightarrow -\infty}^2 \sim \frac{\exp(2\alpha x)}{|x + \text{Re } \delta|^{1/2}} \exp\left[-k \text{Im}\left(\frac{1}{q}\right)x^2\right] \sin^2\left(\frac{2}{3}\left|\frac{x + \text{Re } \delta}{\text{Re } \kappa}\right|^{3/2} + \frac{\pi}{4}\right). \quad (22)$$

If $\text{Re } \kappa < 0$, then $|U|_{x \rightarrow +\infty}^2$ and $|U|_{x \rightarrow -\infty}^2$ correspond to Eqs. (22) and (21), respectively.

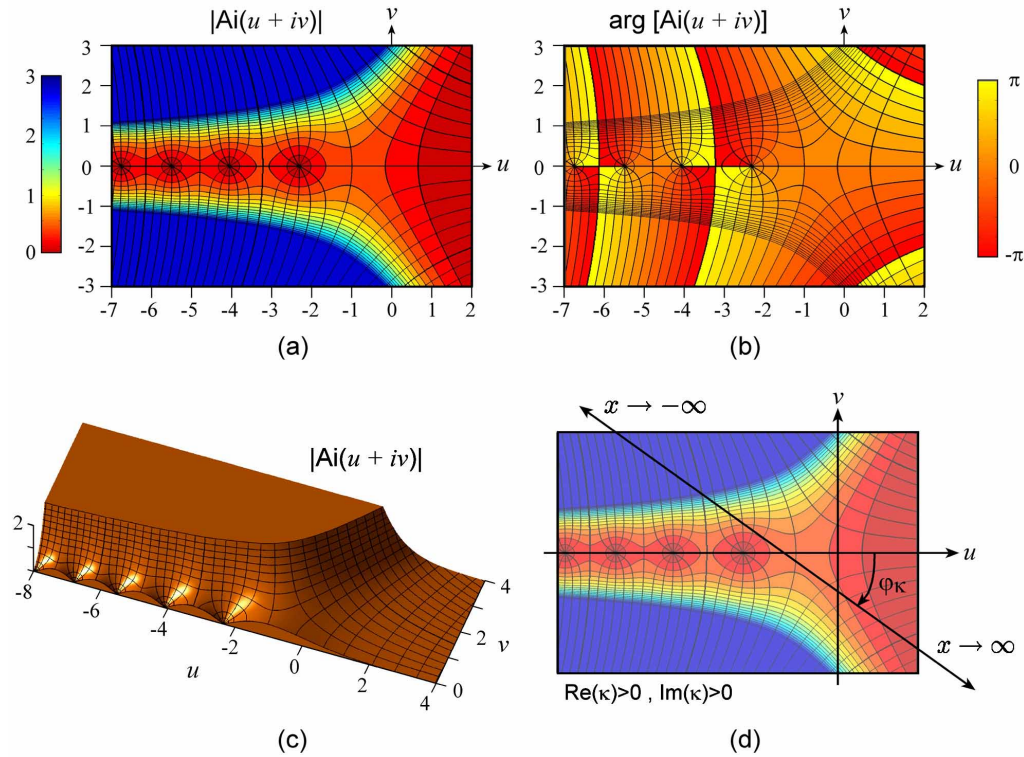


Fig. 3. (a)-(c) Absolute value and phase of the Airy function $\text{Ai}(w)$ on the complex plane $w = u + iv$. (d) The variation of $x \in (-\infty, \infty)$ in the argument of the Airy function $\text{Ai}((x + \delta)/\kappa)$ corresponds to a straight line on the complex $w = u + iv = (x + \delta)/\kappa$ plane. $\phi_\kappa = \arctan[\text{Im}(\kappa)/\text{Re}(\kappa)]$. The figure shows the case $\text{Re} \kappa > 0$ and $\text{Im} \kappa > 0$.

2. When the straight line $v_s(u)$ does not coincide with the real axis $v = 0$. Using Eq. (19) we obtain

$$|U|_{x \rightarrow \pm\infty}^2 \sim \frac{\exp(2\alpha x)}{|x + \delta|^{1/2}} \exp \left[-k \text{Im} \left(\frac{1}{q} \right) x^2 \right] \exp \left[-\cos \left(\frac{3}{2} \varphi \right) \frac{4|x + \delta|^{3/2}}{3|\kappa|^{3/2}} \right], \quad (23)$$

where $\varphi = \arg(w) = \arctan\{[-x \text{Im} \kappa + (\kappa \times \delta)]/[x \text{Re} \kappa + (\kappa \cdot \delta)]\} \in (-\pi, \pi)$, and irrelevant overall constants have been omitted.

From Eqs. (21)–(23) we conclude that the existence of the Gaussian apodization [i.e. $\text{Im}(1/q_1) > 0$] is sufficient for ensuring the square integrability of the AiG beam independently of the values taken by the other constants. Conversely, the condition $\text{Im}(1/q_1) < 0$ causes the field to diverge as $|x| \rightarrow \infty$.

If the initial field is not Gaussian apodized [i.e. $\text{Im}(1/q_1) = 0$], then from Eqs. (21)–(23) we conclude that the beam is still square integrable in the following two symmetrical cases: (a) $\kappa \in \mathbb{R}^+ = (0, \infty)$, $\delta \in \mathbb{R}$, and $\text{Im} S < 0$ (i.e. $\alpha > 0$), (b) $\kappa \in \mathbb{R}^- = (-\infty, 0)$, $\delta \in \mathbb{R}$, and $\text{Im} S > 0$ (i.e. $\alpha < 0$). The case (a) is indeed the required condition to ensure square integrability of the finite-energy Airy beams introduced in Refs. [7, 8].

5. Conclusions

We introduced the AiG beams and demonstrated that these beams can be propagated in a closed and elegant form through paraxial optical systems characterized by ABCD transfer matrices. The propagation of the AiG beams is completely characterized by the transformation of four independent complex parameters. Apart from a complex amplitude factor, the output field has the same mathematical structure as the input field, thus the AiG beams constitute a class of scalar fields whose form is invariant under paraxial optical transformations. The analysis of the first-order moment of the AiG beam confirmed that the position of its centroid through the ABCD system follows the ray trajectory predicted by the geometrical optics. The existence Gaussian apodization is enough to ensure the square integrability of the AiG beam.

Acknowledgments

This research was supported by Consejo Nacional de Ciencia y Tecnología (grant 42808) and by Tecnológico de Monterrey (grant CAT007). M. A. Bandres acknowledge support from the Secretaría de Educación Pública of México. We also acknowledge the help of Cleve Moler, who provided us with an useful Matlab code to generate the plots in Fig. 3.